ARTICLE

Molecular Dynamics Simulation of Hydration Structure of KNO_3 Electrolyte Solution

Gui-wu Lu[a*], Ying-feng Li[a], Wei Sun[a], Chun-xi Li[b]

a. Department of Mathematics and Physics, Petroleum University of China, Beijing 102249, China; b. College of Chemical Engineering, Beijing University of Chemical Technology, Beijing 100029, China

(Dated: Received on June 14, 2006; Accepted on August 8, 2006)

Molecular dynamics simulations were carried out to study the structure of ion clusters and hydration properties of KNO_3 solution. The water molecule was treated as a simple-point-charge (SPC) model, and a four-site model for the nitrate ion was adopted. Both the Coulomb and Lennard-Jones interactions between all the charged sites were considered, and the long-range Coulomb electrostatic interaction was treated using Ewald summation techniques. The configuration of ionic pairs, the radial distribution function of the solution, and the effect of solution concentration on ionic hydration were studied in detail. It was found that there are ionic association phenomena in KNO_3 solution and that the dimeric, triplet, solvent-separated ion pairs, and other complex clusters can be observed at high ionic concentration condition. As the concentration of solution decreases, the ionic hydration number increases, 5-7 for cation K^+ and 3.5-4.7 for anion NO_3^-, which is in good agreement with former Monte Carlo and time-of-flight neutron diffraction results.

Key words: KNO_3, Electrolyte solution, Ionic hydration, Molecular dynamics

I. INTRODUCTION

Electrolyte solutions are of great significance for many practical systems and industrial processes such as room temperature ionic liquids, colloid systems, electrochemical processes, homogeneous and nonhomogeneous catalysis, separation of salt-containing systems, and crystal growth processes [1-10]. However, the elucidation for electrolyte solution systems remains partially unclear [11,12]. There are many questions about the development of exact liquid state theory due to the long-range nature of the electrostatic forces and the lack of a credible structural model [13-18]. These difficulties are, to some extent, solved by using computer simulation, which is able to give exact answers for many aspects of the behavior of defined models of the liquid state [19-21]. The computer simulation techniques can provide detailed information in the neighborhood of the molecules or macromolecules at nonhomogeneous interfaces, or around ions in solution using the usual radial distribution function or multivariable distribution functions [10,11,22].

It has been a matter of interest for a long time to elucidate the hydration structure of the nitrate ion, NO_3^-. The hydration structure of NO_3^- has been investigated by X-ray diffraction for concentrated NH_4NO_3 and $NaNO_3$ aqueous solutions [23,24]. It is difficult, however, to deduce the detailed hydration structure of NO_3^- from the X-ray diffraction data alone, because several interatomic correlations overlap in the range of the radial distance, $2<r<4$ Å, where the NO_3-H_2O correlation should be contained [25]. In particular, the information on the orientational configuration between NO_3 and the surrounding H_2O molecules cannot be given from the X-ray diffraction measurement owing to the extremely weak scattering power of hydrogen atoms.

Much clearer structural information has been supplied through a neutron diffraction study for a $NaNO_3$ solution by the $^{14}N/^{15}N$ isotopic substitution technique, and the results indicate that a strong hydrogen bond between N and D atoms is formed in the aqueous solution [26]. However, experiments on concentrated ND_4NO_3 and $LiNO_3$ solution give no indication of the pronounced first peak. It seems that there still remain some uncertainties on the hydration structure of NO_3 in the aqueous solution [25].

In this work, the simple-point-charge (SPC) water model was adopted, and the hydration structure of KNO_3 electrolyte solution was investigated using molecular dynamics simulation.

II. MOLECULAR MODEL

The potassium cation was treated as a charged sphere, and water molecule is treated as SPC model. The nitrate anion was treated as a rigid, planar entity with C_3 symmetry which embodies four fractional charges, one on each atom, and a net charge of one electron on the whole ion. The fractional charges were obtained from a Mulliken population analysis of an *ab initio* self-consistent-field (SCF) molecular orbital calculation of the isolated gas phase anion, which is described in detail in earlier Monte Carlo studies [27,28]. The related parameters are presented in Table I.

*Author to whom correspondence should be addressed. E-mail: lugw@cup.edu.cn, Fax: +86-10-69744849

TABLE I Force field parameters for species in KNO_3 electrolyte solution[a]

Species	σ/Å	Partial charges	Bonding length/Å	ε/K
N	3.10	0.198	–	37
O(NO_3^-)	3.00	−0.399	–	37
N−O	–	–	1.302	
K	2.76	1.00	–	0.08
H(H_2O)	–	0.41	–	–
O(H_2O)	3.17	−0.82	–	0.15
H−O	–	–	1.00	–

[a] σ and ε are L-J parameters, and they are cited from Refs.[29] and [30].

The systems considered here are composed of N_+ potassium cations, N_- nitrate anions and N_w water molecules. Based on the pair-wise additivity, the configuration energy U of the solution can be written as

$$U = \frac{1}{2} \sum_{\alpha=\{+,-,w\}} \sum_{\gamma=\{+,-,w\}} \sum_{k=1}^{N_\alpha} \sum_{l=1}^{N_\gamma}{}' u_{\alpha\gamma}(kl) \qquad (1)$$

where $u_{\alpha\gamma}(kl)$ is the pair potential between particle α and γ corresponding to distance r_{kl}, and the prime symbol on the last summation requires that $k \neq l$ when $\alpha=\gamma$. The interaction energy for a pair of molecules (or ions) i and j consists of the Coulomb and Lennard-Jones interaction between all the charged sites:

$$u_{ij}(r) = \sum_{\alpha=1}^{n_a} \sum_{\beta=1}^{n_b} \left\{ 4\varepsilon_{\alpha\beta} \left[\left(\frac{\sigma_{\alpha\beta}}{r_{\alpha\beta}} \right)^{12} - \left(\frac{\sigma_{\alpha\beta}}{r_{\alpha\beta}} \right)^{6} \right] + \frac{{z_i}^{\alpha} {z_j}^{\beta} q^2}{4\pi\varepsilon_0 r_{\alpha\beta}} \right\} \qquad (2)$$

where ${z_i}^{\alpha}$ is the fractional charge on site α of ion i, q is the charge of a proton, $r_{\alpha\beta}=|\mathbf{r}_\alpha - \mathbf{r}_\beta|$ is the distance between site α and β, σ and ε are L-J parameters. As shown in Table I, the potential parameters for water and KNO_3 were taken from Laaksonen *et al.* [29] and Benendsen *et al.* [30]. The cross-interaction terms were constructed using the so-called Lorentz-Berthelot combination rules [31,32].

The long-range Coulomb electrostatic interactions between charge i and j were treated using Ewald summation techniques. The convergence parameter κ, real-space cut distance r_{cut} and reciprocal maximum vector K_{max} were chosen as 5.8 L, 0.5 L and 3, respectively, according to former work for parameter optimization of the Ewald summation [33]. The minimum image convention was used together with periodic conditions to maintain constant density and to prevent condensation at walls of the simulation cell. In this work ten state points were simulated, which correspond to different temperatures and concentrations, and accordingly different reduced densities. The concentration c, with units of mol/L, is calculated with Eq.(3) by using the experimental density d of KNO_3 aqueous solution [34], at specified temperature.

$$c = \frac{dx1000}{M_{KNO_3}} \qquad (3)$$

where x and M are mass fraction of KNO_3 in the solution and molar mass of KNO_3 respectively. The simulation conditions are specified by temperature T and concentration c, which is listed in Table II, where total ionic number $N_i=N_+ + N_-$.

TABLE II The simulation conditions for different state points (N=864)

State	c/(mol/L)	x/%	d/(g/cm^3)	T/K	N_i
A	0.302	4	1.023	303	14
B	0.611	8	1.050	303	26
C	0.834	16	1.100	303	54
D	1.622	24	1.161	303	88
E	3.732	33	1.228	303	128
F	1.598	16	1.084	333	54
G	2.839	24	1.142	333	88
H	4.249	34	1.219	333	136
I	5.859	45	1.317	333	190
J	6.994	52	1.387	333	248

Microcanonical ensemble (NVE) molecular dynamics simulations were performed for the systems in Table II. The initial configuration is generated from a face-centered cubic (FCC) lattice by assigning the ions and water molecules randomly to its lattice sites. Both molecular species, i.e. water and nitrate, were kept rigid throughout the simulations and the equations of motions were solved using leapfrog scheme with a timestep of 1 fs. The pre-equilibrium period was performed for 800 ps, and the data collection was then performed for 1000 ps. The simulations were performed with a modified version of the simulation program of Mcmoldyn package [35].

III. RESULTS AND DISCUSSION

A. Structure of KNO_3 solution

The water-water radial distribution functions, $g_{O-O}(r)$, $g_{O-H}(r)$ and $g_{H-H}(r)$ for three states (F, H and J) at the temperature, 333 K, are shown in Fig.1. Water in a mixture seemed less structured than pure water. Many monatomic ions tend to break the structure of the water surrounding them, thus are called structure breakers [29]. Hydro-phobic solutes tend to enhance the water structure exerting structure-making effects on water. In the case of a mixture of potassium cations and polyatomic nitrate anions, the sol-

ISSN 1003-7713/DOI:10.1360/cjcp2007.20(1).22.9

vation mechanism is an interplay of different types of interactions, therefore it is impossible to rationalize in simple terms [29].

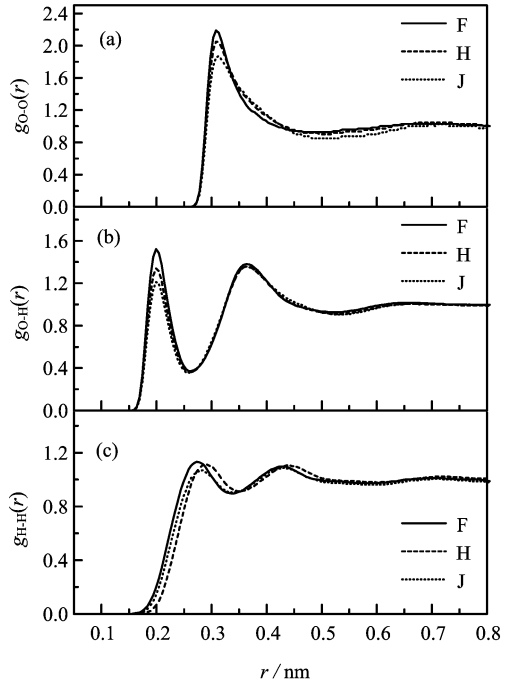

FIG. 1 Radial distribution function (RDF) for water-water of KNO_3 solution in different ion concentrations at 333 K. The solution concentration of KNO_3 for states F, H, and J is 1.598, 4.249, and 6.994 mol/L, respectively. (a) Oxygen-oxygen radial distribution functions. (b) Oxygen-hydrogen radial distribution functions. (c) Hydrogen-hydrogen radial distribution functions.

The characteristic second maximum of $g_{O-O}(r)$ near 0.45 nm, reflecting the tetrahedral ordering of water molecules due to hydrogen bonding, is completely absent in the mixture, and a pronounced minimum of the distribution appears in its place (see Fig.1(a)). The comparison of $g_{O-O}(r)$ functions at different ion concentrations shows a significant decrease of the first peak for concentrated solution, and the first minimum location shifts from 0.45 nm to 0.52 nm as the concentration increases from 3.7 mol/L to 7.0 mol/L. In other words, as the ion concentration increases, some water molecules are redistributed from hydrogen-bonding regions of approximately 0.32 nm to non-bonding regions of 0.45 nm. It has been previously shown that the pairs of molecules at intermediate distances are primarily responsible for repulsive interactions in liquid water [36,37], and these repulsion interactions obviously decrease for concentrated solutions.

The sharp first peak (at 0.20 nm) of $g_{O-H}(r)$ becomes less pronounced under high ion concentration conditions (Fig.1(b)). This characteristic peak of $g_{O-H}(r)$ observed in computer simulations, as well as experimentally, is the basis of a simple geometric definition of a hydrogen bond. The hydrogen bond is assumed to exist between any pair of H_2O molecules whose respective O and H atoms are separated by a distance less than R_{HB}=0.26 nm [38]. Integration under $g_{O-H}(r)$ up to the chosen threshold distance (first minimum) provides a convenient way to quantitatively estimate the average number of H-bonds $\langle n_{HB}\rangle$. In our simulation conditions, $\langle n_{HB}\rangle$ can be expressed as

$$\langle n_{HB}\rangle = 4\pi\rho_H \int_{0.15}^{0.26} g_{O-H}(r) r^2 dr \qquad (4)$$

where ρ_H is number density of H atom in KNO_3 solution. The corresponding results are listed in Table III. Using linear extrapolation, we obtain $\langle n_{HB}\rangle$ for pure water is 3.16 at 303 K, which is in good agreement with that of Kalinichev *et al.* [38]. It is found that the average amount of H bonding decreases with ion concentration increase (Table III), which indicates the KNO_3 is a species which destroys H-bonding.

TABLE III The average number of H-bonds in KNO_3 solution

Temperature/K	State	$\langle n_{HB}\rangle$
303	A	3.10
	B	3.04
	C	3.01
	D	2.97
	E	2.95
333	F	2.66
	G	2.62
	H	2.58
	I	2.55
	J	2.51

Figure 2 shows the water-ion radial distribution function for state F. Symbols O_W and O_N, hereafter, represent oxygen atoms of water and nitrate respectively. The hydration number for K^+ is estimated to be from 4.0 to 7.0 depending on the method used in the estimation. The first very sharp peak of the simulated $g_{O_W-K^+}(r)$ shown in Fig.2 contains 5.4 water-oxygens when integrated to the first minimum at 0.36 nm. The radial distribution function between the oxygen atom of water and the nitrogen atom shows a maximum at 0.4 nm, indicating that the water molecules do not closely coordinate with the nitrogen but rather with the oxygen of the nitrate. From RDF curves $g_{O_W-N}(r)$ we can calculate up to five water molecules in the first hydration shell around the nitrate by integrating to the first minimum at 0.46 nm. According to a neutron diffraction study for $NaNO_3$ solutions [26], there total exist five coordinated water molecules for NO_3^-, both axially (r_{NOw}=0.265 nm) and radially (r_{NOw}=0.340 nm), in the first hydration shell, which is in good agreement with our output. Figure 2(b) shows the corresponding radial distribution functions

ISSN 1003-7713/DOI:10.1360/cjcp2007.20(1).22.9

between the hydrogen and ions. The hydrogen atoms are found with the first maximum at 0.36 nm around the potassium ion. The $g_{O_N-H}(r)$ curve shows a very strong hydrogen bond structure with the first maximum at 0.185 nm followed by a broader second maximum due to the second hydration shell (which is not involved in the hydrogen bond with the nitrate). The second maximum also contains a weaker subsidiary peak, which results from the interaction between the hydrogen atom of water and the oxygen atom of nitrate.

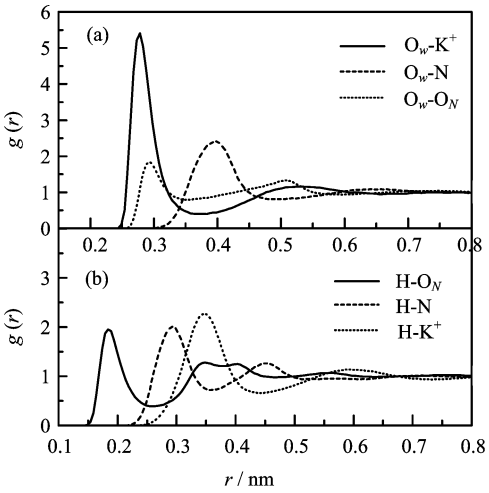

FIG. 2 The radial distribution function between the ion sites and water sites for state F at 333 K with concentration of 1.598 mol/L. (a) Oxygen-potassium, oxygen-nitrogen and oxygen-oxygen radial distribution functions. (b) Hydrogen-oxygen, hydrogen-nitrogen, and hydrogen-potassium radial distribution functions.

Figure 3 shows the radial distribution functions for K−K, K−N and K−O_N pairs, respectively, between the ions. Each figure contains the RDF curves for three different concentration solutions (F, H and J) in a direct comparison. Though there is considerable uncertainty in the pair correlation function between cations, $g_{K-K}(r)$, a weak maximum near 0.45 nm does appear in states F and H, as shown in Fig.3(a), which indicates the formation of nearly nonlinear triplet configurations (K−NO_3−K triplet). The large uncertainty near 0.45 nm for the high concentration solution (state J) is a consequence of the presence of a pair of triplets, both the linear and nonlinear (+−+) configuration, which persisted for very large segments of the MD phase space. It is interesting to find from Fig.3(a) that the nonlinear (+−+) triplet configurations decrease rapidly as the solution becomes more concentrated. These results are in agreement with the observation in Fig.2. The peaks located between 0.6 and 0.8 nm correspond to the solvent separated triplet configuration, which will be discussed with more detail in terms of the ionic hydration.

It is seen that, as shown in Fig.3(b), the first peak enhances as the concentration increases from 1.598 to 6.994 mol/L. At the highest ion concentration we ob-

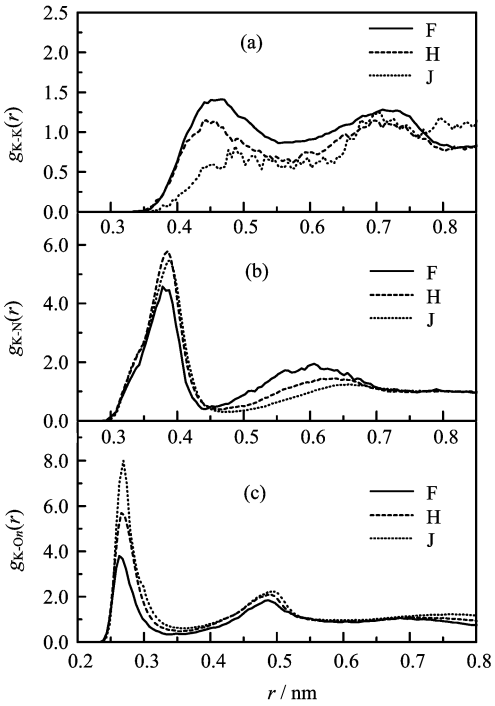

FIG. 3 The radial distribution functions for (a) K−K, (b) K−N and (c) K−$O(NO_3)$ pairs at 333 K. The solution concentration of KNO_3 for states F, H and J is 1.598, 4.249, and 6.994 mol/L, respectively.

serve the strongest structure. The formation of cation-anion ion pairs is indicated by the height of the first and second maximum in $g_{N-K}(r)$ near 0.38 and 0.60 nm, corresponding to the ionic pairs through K−N and K−O_N bonding respectively. At higher concentrations the second shell maxima are reduced in height and broadened, which indicates a negative effect of ion concentration on the formation of solvent separated cation-anion ion pairs. To learn more about the concentration dependence of the ionic environment, we determine the number of particles of type α around a central cation in a spherical shell r_1 to r_2

$$\Gamma_\alpha(r_1, r_2) = 4\pi\rho_\alpha \int_{r_1}^{r_2} r^2 g_{+\alpha}(r)\mathrm{d}r \qquad (5)$$

From Eq.(5) and $g_{K-N}(r)$, values of $\Gamma_{NO_3^-}$ between the second and third minima in $g_{K-N}(r)$ for states F through J were calculated as 0.3, 0.5, 0.8, 1.2 and 1.8, respectively. This means that the local ion density near the third peak (this peak is not shown in Fig.3) of the $g_{K-N}(r)$ function is enhanced with the increase of ion concentration in electrolyte solution. As ion concentration increases, the depth of the minimum for the mean force potential between an ion pair sharing a common solvent molecule is diminished relative to other potential surface features [36]. The rigid linearity and permanence of these triplet configurations is lost as the potential well is broadened. The apparent enhancement

ISSN 1003-7713/DOI:10.1360/cjcp2007.20(1).22.9

of ion cluster size at higher concentration arises as a consequence of the increased relative mobility and local ionic densities.

It is seen that the variation of $g_{K-O_N}(r)$ with concentration, as is shown in Fig.3(c), is more regular than g_{K-N}, and the first and second peaks appear higher as the concentration increases from 1.598 to 6.994 mol/L. It is noted that the first maxima of $g_{K-O_N}(r)$ located near 0.26 nm increases from 4 to 8 as the concentration of electrolyte solution increases from 1.598 (F) to 6.994 (J) (in mol/L). This suggests that there is a rather high degree of ionic association in these systems, and that the dimer fraction is obviously enhanced as the solution becomes more concentrated. The second peak located near 0.48 nm indicates that the K^+ is arranged in the bisector of the ONO angle of NO_3^- and the formation of $K-NO_3^-$ pairing which has more compact structure. This arrangement was also found to give the lowest configuration energy in static calculation [39]. As the solution becomes more concentrated, the height of the second peak has a slight enhancement (see Fig.3(b)), indicating that the fraction of K-NO_3 pairing increases with the increase in concentration, which agrees well with previous observations by Eggebrecht and Ozler [22]. Figure 4 shows the structural pair correlations between the nitrate sites N−N, N−O_N, and O_N−O_N. In the dilute solution there is hardly any structure to be observed between the nitrate sites, since they are strongly hydrated by the water. All the simulated ionic pair distribution function in Fig.1-Fig.4 for KNO_3 solution are very similar to the ones obtained by Laaksosen *et al.* [29] in their MD work for $AgNO_3$.

We examined the size distribution of ionic clusters in different systems. In a cluster, each site is connected, either directly or indirectly, to sites of other particles. The directly or indirectly connected sites are determined by the same method used in the literature [27,28,40]. Figure 5 shows the ion cluster size distribution for states F-H at 333.15 K, which clearly indicates the decrease of solitary ion population as well as the broadening distribution of ionic clusters with increasing ion concentration. For state F with low ionic concentration, the ion cluster is mainly composed of single, dimeric and tri-ion clusters along with very small fraction of 4-mer clusters. For state I, 12, 18 and 21-mer clusters were also obtained, which did not follow charge neutrality. State point J has a broader distribution of ionic clusters between 29 and 73-mer, which is not shown in Fig.5. These large clusters are serpentine and formed by the association of ions of alternating charge, which is in agreement with former Monte Carlo findings [27].

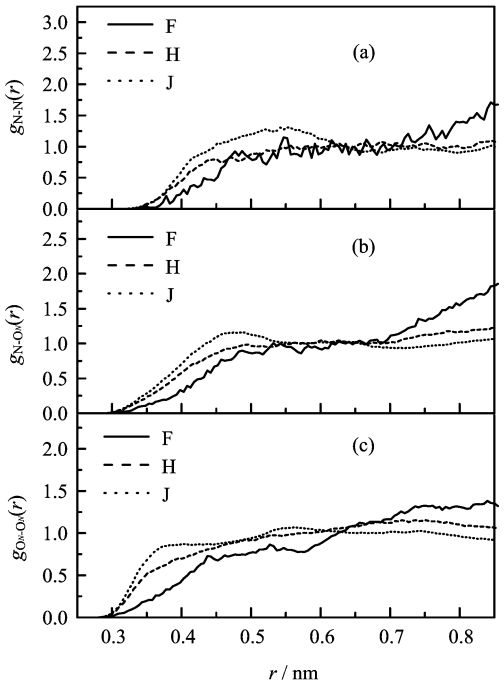

FIG. 4 The radial distribution functions between the nitrate sites for (a) N−N, (b) N−O_N and (c) O_N−O_N. The solution concentration of KNO_3 for states F, H, and J is 1.598, 4.249, and 6.994 mol/L, respectively.

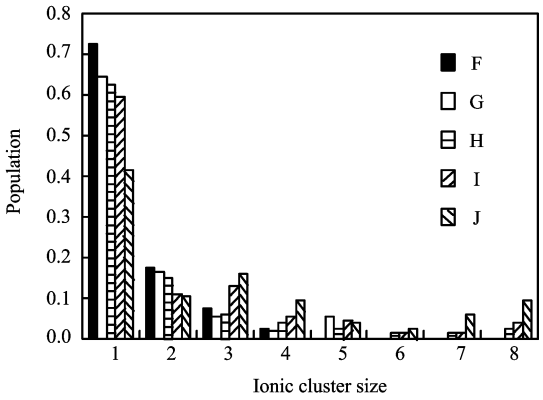

FIG. 5 Distribution of ionic cluster for states F-J at 333 K. The solution concentration of KNO_3 for states F, G, H, I and J is 1.598, 2.839, 4.249, 5.859 and 6.994 mol/L, respectively.

B. The hydration structure of the ion pairs

The ion pair's configuration was examine in KNO_3 solution in more detail. In a condensed phase, the ion association process may be described in terms of an equilibrium between two states of the associated ions: the contact ion pair (CIP) and the solvent-separated ion pair (SSIP). The interconversion between the two states for charged ions in a pair at room temperature would involve passing over a free energy barrier. The resulting potential curve for an ion pair in solution can be obtained by the simple conversion of the RDF into the mean force potential (MFP) [41]:

$$w(r) = -kT \ln[g(r)] \tag{6}$$

The MFP for the ion pairs is displayed in Fig.6 with

ISSN 1003-7713/DOI:10.1360/cjcp2007.20(1).22.9

the two minima, CIP and SSIP, separated by a barrier for any ion species in different ion concentration. Barrier crossing may be considered as an activated process driven by solvent fluctuations [42]. The presence of this free energy barrier is the result of cancellation between the bare interionic interaction and the reaction field provided by the solvent that tends to separate the two ions. At short distances, the final shape of the potential of mean force depends mainly on the local structure of the solvent surrounding the ion pair. From the microscopic point of view, the SSIP-CIP process involves expelling solvent molecules from the region lying between the two ions into the bulk solvent.

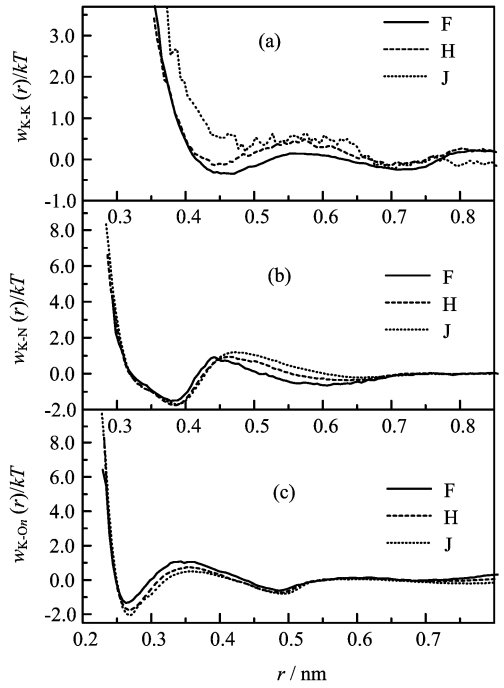

FIG. 6 The mean force potential (MFP) as a function of the interionic distances at 333 K. The solution concentration of KNO_3 for states F, H and J is 1.598, 4.249 and 6.994 mol/L, respectively. (a) Potassium-potassium. (b) Potassium-nitrogen. (c) Potassium-oxygen.

In the K-K case, two "distinctly" separated minima are observed in contrast to previous simulations. For state F, a potential barrier on the order of $0.4kT$ separates them. For states H and J, the barrier is around $0.30kT$ and $0.1kT$, respectively, indicating a dramatic decrease in potential well height with the ion concentration. In the highest ion concentration solution (state J), the average force potential shows an oscillatory behavior, which might be interpreted as the formation of relatively stable ion pairs at short interionic distances. This observation reinforces the amazingly high fraction found for the solvent-separated K-K pairs. Comparing the curves in Fig.6(b), one can see that the energy barrier between the first minimum and maximum points increases from $2.5kT$ to $3kT$ as the concentration grows from 1.6 mol/L to 7.0 mol/L, while the second potential well becomes lost and broad in the high ion concentration condition. These observations suggest the solvent separated cation-anion pairs become instable and the fraction of contact dislike ion pair increases significantly in the condensed ion solution. It is interesting to find from Fig.6(c), that the energy barrier for CIP and SSIP transition is almost the same for different ion concentration solutions, and its height is about $2.3kT$, which is much smaller than that for the K-N ion pair case. Thus we can concluded that dislike ion pair is more apt to form through the oxygen atom of NO_3 than through the nitrogen atom.

A snapshot from state F is displayed in Fig.7, in which a contact K-NO_3 pair and a solvent separated K-NO_3 pair are shown with more detail. There is a hydrogen bond network around the K-NO_3 pair. Such a network is possible only at small ion-pair separation and may certify the locally stable contact ion-pair arrangement. The snapshot does not show direct interaction between K ions in the KNO_3 solution. In contrast, favorable interaction between hydrated cations is possible, while the hydrogen forms an H-bond with the oxygen atom of nitrate. The water-nitrate hydrogen bond has been pointed out to be remarkably stable. In conclusion, the hydrogen bond within the ion-pair and/or small hydrates thereof may be an important factor for stabilizing the contact form as compared to the solvent separated one. The ion pair configuration as well as their hydration structure is shown in Fig.8.

The simplest case is the hydration of the K-K pairs, where they can divide appropriately the two free elec-

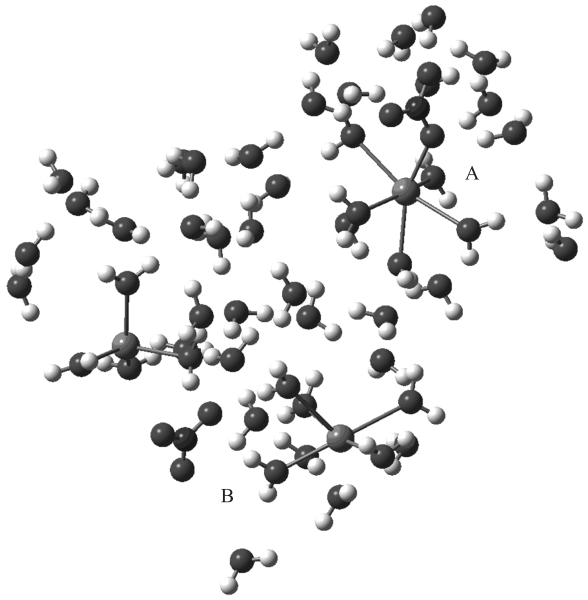

FIG. 7 A structure snapshot of KNO_3 solution for state F with the lowest ion concentration 1.598 mol/L. A contact K-NO_3 pair and a solvent separated K-NO_3 pair are notated with symbol "A" and "B", respectively.

ISSN 1003-7713/DOI:10.1360/cjcp2007.20(1).22.9

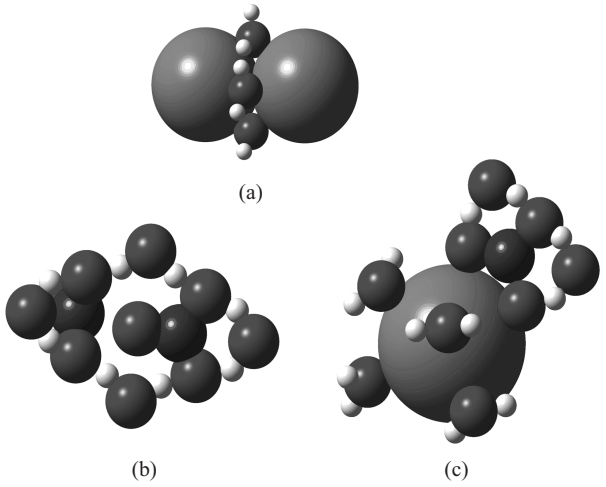

FIG. 8 The ion pair configuration and hydration structure. (a) K-K pair, (b) NO_3-NO_3 pair, (c) K-NO_3 pair.

tron pairs of the oxygen atoms of water. The resulting structure is also symmetric with a dihedral angle equal to 72°, suggesting a $[2K^+(H_2O)_5]$ description for the K-K pairs (see Fig.8(a)). The hydrogen atoms of the common water molecule (CWM) are directed properly to the bulk being able to form hydrogen bonds. For the hydration of the NO_3-NO_3 pairs, two hydrogen atoms of the CWM are attracted to the two oxygen atoms of the NO_3 group, while the oxygen atom of the CWM is located at 0.304 nm from the interionic axis. The most probable CWM-CWM distance is 0.475 nm so that the dihedral angle between the two anion planes is about 90°. These results suggest that in the ideal situation, the NO_3-NO_3 pairs can be described by $[2NO_3(H_2O)_2]$ configuration. The simplicity of this structure is obviously related to the easy removal of water molecules and to the sharing of the CWM without deeply breaking the hydration structure of each ion. The ability to approach two hydrated ions with the consequent sharing of hydration molecules is not observed in the case of K^+, since they are unable to attract the same water molecule simultaneously. In the K^+-NO_3^- pairs, the CWM is closer to the K^+ than NO_3 group, and its position corresponds exactly to a dihedral angle (between the plane containing both cation and anion ion and one CWM) of 90°.

The orientation variation of a water molecule around a central cation and anion at 333 K was further investigated in terms of average cosine of orientational angle between the vector of dipole moment (here the vector is from the oxygen to the midpoint of the two hydrogens in the water molecule) and the radial vector of an ion-Ow pair $\mathbf{r}_{ij}$, which can be calculated with Eq.(7)

$$\cos\theta = \frac{{r_{13}}^2 - {r_{12}}^2 - {r_{23}}^2}{2r_{12}r_{23}} \tag{7}$$

where r_{12}, r_{13} and r_{23} are the distances between central ion 1 and oxygen atom 2 of the water molecule, central ion 1 and midpoint 3 of the two hydrogen atoms of the water molecule, and the oxygen atom and midpoint of the two hydrogen atoms in water molecules, respectively. Figure 9 displays the mean cosine of SPC water molecule orientation around the NO_3 group for states G, H, I and J, in which high concentration states show rapid reduction of orientational ordering with increasing ion-solvent separation. It is obvious that the solvent is highly oriented in the vicinity of an ion, and that the water molecule approaches random orientation at longer separation distances. The strong orientation suggests an ionic hydration phenomenon in the first coordination layer of a central ion, which is the physical basis for some semi-empirical models of electrolyte solution based on the ionic hydration assumption. It is seen that the ionic hydration structure is similar at different ionic concentrations and the lower the ionic concentration, the thicker the solvation layer, provided that the distance, at which the average cosine drops to zero can be taken as an indicator of the hydration shell thickness. This variation is in accordance with the experimental findings on ionic hydration number [43].

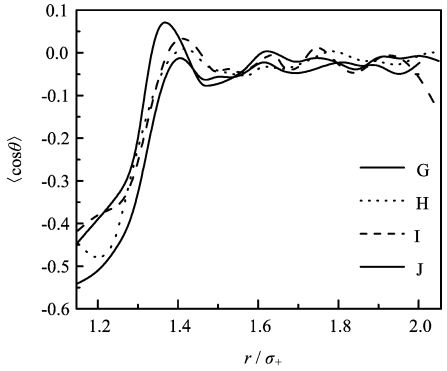

FIG. 9 The mean cosine of SPC water molecules orientation around NO_3 group for state G, H, I and J at 333 K. The concentration for states G, H, I and J are 2.839, 4.249, 5.859 and 6.994 mol/L, respectively.

The separation $r{=}r_s$ where $g_{\mathrm{ion-Ow}}(r)$ has its first minimum may be defined as the first coordination shell of the central ion, and integration of $4\pi\rho_W r^2 g_{\mathrm{ion-Ow}}(r)$ up to this point yields the coordination number n_{ion}. The coordination numbers thus calculated, as well as the previous Monte Carlo results and experimental results for K^+ and NO_3^- for anion are listed in Table IV. Obviously, the Table IV results are in excellent agreement for K^+ and in good agreement for NO_3^-. Besides this, their variation trend with concentration is in qualitative agreement. For smaller ions (Li^+, Na^+), n_{ion} is a well-defined quantity since the integral plateaus as a function of its upper limit and the precise choice of outer radius of the coordination shell is unimportant [48]. In the case of K^+ and NO_3^-, the RDF has a much shallower first minimum, so there are some deviations in the

ISSN 1003-7713/DOI:10.1360/cjcp2007.20(1).22.9

TABLE IV First shell coordination number of ions

System	K^+			NO_3		
	This work	MC[a]	Literature value[b]	This work	MC[a]	Literature value[b]
F	7.2	7.3	7.8	4.9	4.7	∼4.3
G	7.1	6.9	7.0	4.7	4.3	∼4.2
H	6.8	6.6	6.3	4.2	4.0	–
I	6.5	6.4	5-7	4.0	3.5	∼3.0
J	6.1	5.5	4-6	3.6	3.2	–

[a] MC results see Refs.[27] and [28].
[b] Literature results for hydration number of K^+ and NO_3^- see Refs. [44-46] and [23-26], [47] respectively.

determination of n_{ion} since the penetration of molecules belonging to the second shell of neighbors will result in an overestimation for hydration number if an arbitrary cut is made. This may be the reason for the deviation between the simulation and experimental results.

IV. CONCLUSION

Molecular dynamics computer simulation for KNO_3 solution is carried out in the concentration range from 0.3 to 7.0 mol/L. The structure parameters and charge distribution of anion NO_3^- are determined via *ab initio* calculations at the self-consistent field (SCF) level. The cation (K^+) is regarded as a charged sphere, solvent water molecules are handled with a simple-point-charge (SPC) model, and a simple four-site model for the nitrate ion is adopted in this study. By simulating relatively large systems for long sampling periods, quantitatively useful results have been obtained. First, the population of solitary ions decreases with increasing ion concentration. As ion concentration increases the distribution of n-mers broadens. Much larger ion clusters, such as 29- and 73-mers, are observed in supersaturated solutions at a temperature of 333 K. Secondly, the idealized structures of all pairs include two to five water molecules located in such a way that the attractive energies are increased and the repulsive ones decreased. Finally, solvent molecules sheathe the ionic cluster, and the thickness of the first ionic hydration shell decreases with increasing concentration. It is found that with the decreasing of solution concentration, the ionic hydration number varies from 5-7 for cation K^+ and 3.5-4.7 for anion NO_3^-, which is in good agreement with former Monte Carlo and experimental results. The satisfactory results presented here for KNO_3 solution encourage further study of the stability of ionic pairs, hydration dynamics and structure relaxation process.

V. ACKNOWLEDGMENTS

This work was supported by the CNPC Innovation Foundation (04E7038), the Natural Science Foundation of Shandong Province of China (Y2003A01) and the Scientific Research Foundation of the Petroleum University of China. We want to thank Professor A. Laaksonen for valuable discussions.

[1] L. Degreve and M. Lozada-Cassou, Phys. Rev. E **57**, 2978 (1998).
[2] J. Yu, L. Degreve and M. Lozada-Cassou, Phys. Rev. Lett. **79**, 3656 (1997).
[3] M. Yamagami, H. Wakita and T. Yamaguchi, J. Chem. Phys. **103**, 8174 (1995).
[4] T. Yamaguchi, M. Yamagami, H. Ohzono, H. Wakita and K. Yamanaka, Chem. Phys. Lett. **252**, 317 (1996).
[5] C. X. Li, R. Tian, G. W. Lu, Z. H. Wang and W. C. Wang, Acta Chim. Sin. **61**, 175 (2003).
[6] G. W. Neilson and J. E. Enderby, J. Phys. Chem. **100**, 1317 (1996).
[7] C. X. Li, Y. G. Li and J. F. Lu, Acta Chim. Sin. **58**, 1349 (2000).
[8] P. Jungwirth, J. Phys. Chem. A **104**, 145 (2000).
[9] T. Asada and K. Nishimoto, Chem. Phys. Lett. **232**, 518 (1995).
[10] L. Degreve and F. L. B. da Silva, J. Chem. Phys. **110**, 3070 (1999).
[11] F. L. B. da Silva, W. Olivares-Rivas, L. Degreve and T. Akesson, J. Chem. Phys. **114**, 907 (2001).
[12] P. I. Nagy and K. Takacs-Novak, J. Am. Chem. Soc. **122**, 6583 (2000).
[13] C. X. Li, H. Y. Song, Y. G. Li and J. F. Lu, J. Chem. Ind. Eng.(China) **52**, 363 (2001).
[14] Y. G. Li, Tsinghua Science and Technology **9**, 444 (2004)
[15] V. A. Payne, J. H. Xu, M. Forsyth, M. A. Ratner, D. F. Shriver and S. W. de Leeuw, J. Chem. Phys. **103**, 8734 (1995).
[16] V. A. Payne, J. H. Xu, M. Forsyth, M. A. Ratner, D. F. Shriver and S. W. de Leeuw, J. Chem. Phys. **103**, 8746 (1995).
[17] I. M. Svishchev and P. G. Kusalik, Phys. Rev. Lett. **73**, 975 (1994).
[18] D. Laria and R. F. Fernandez-Prini, Chem. Phys. Lett. **205**, 260 (1993).
[19] J. Zhou, X. H. Lu, Y. R. Wang and J. Shi, J. Chem. Ind. Eng.(China) **51**, 143 (2000).

ISSN 1003-7713/DOI:10.1360/cjcp2007.20(1).22.9

[20] J. Zhou, Y. Zhu, W. C. Wang, X. H. Lu, Y. R. Wang and J. Shi, Acta Phys. Chim. Sin. **18**, 207 (2002).
[21] P. G. Kusalik and G. N. Patey, J. Chem. Phys. **88**, 7715 (1988).
[22] J. Eggebrecht and P. Ozler, J. Chem. Phys. **98**, 1552 (1993).
[23] R. Caminiti, G. Licheri, G. Piccaluga and G. Pinna, J. Chem. Phys. **68**, 1967 (1978).
[24] R. Caminiti, G. Licheri, G. Piccaluga and G. Pinna, J. Chem. Phys. **72**, 4522 (1980).
[25] Y. Kameda, H. Satoh and O. Uemura, Bull. Chem. Soc. Jpn. **66**, 1919 (1993).
[26] G. W. Neilson and J. E. Enderby, J. Phys. C: Solid State Phys. **15**, 2347 (1982).
[27] G. W. Lu, C. X. Li, W. C. Wang and Z. H. Wang, Mol. Phys. **103**, 599 (2005).
[28] G. W. Lu, C. X. Li, W. C. Wang and Z. H. Wang, Fluid Phase Equilibria **225**, 1 (2004).
[29] A. Laaksonen and H. Kovacs, Can. J. Chem. **72**, 2278 (1994).
[30] H. J. C. Berendsen, J. P. M. Postma, W. F. van Gunsteren and J. Herman, *In Intermolecular Forces*, Holland: Reidel, Dordrecht, 331 (1981).
[31] H. A. Lorentz, Ann. Phys. **12**, 127 (1881).
[32] D. Berthelot and C. R. Hebd, Seances Acid. Sci. Paris, 1703 (1898).
[33] G. W. Lu, C. X. Li, W. C. Wang and Z. H. Wang, Chin. J. Chem. Phys. **17**, 547 (2004).
[34] O. Sohnel and P. Novotny, *Density of Aqueous Solution of Inorganic Substance*, Oxford: Elsvier, (1985).
[35] A. Laaksonen, Comput. Phys. Commun. **42**, 271 (1986).
[36] A. G. Kalinichev and J. D. Bass, J. Phys. Chem. A **101**, 9720 (1997).
[37] H. Tanaka and I. Ohmine, J. Chem. Phys. **87**, 6128 (1987).
[38] A. G. Kalinichev, Mineralogical Society of America **42**, 81 (2001).
[39] W. Smith and J. H. R. Clarke, J. Chem. Phys. **90**, 6610 (1989).
[40] E. M. Sevick, P. A. Monson and J. M. Ottino, J. Chem. Phys. **88**, 1198 (1988).
[41] T. L. Hill, *Statistical Mechanics*, New York: McGraw-Hill, 1956.
[42] C. Dedonder-Lardeux, G. Gregoire, C. Jouvet, S. Martrenchard and D. Solgadi, Chem. Rev. **100**, 4023 (2000).
[43] C. H. Fang, Progress in Chemistry (in Chinese), **8**, 318 (1996).
[44] E. Clementi and R. Barsotti, Chem. Phys. Lett. **59**, 21 (1978).
[45] M. Mezei and D. L. Beveridge, J. Chem. Phys. **74**, 6902 (1981).
[46] F. T. Marchese and D. L. Beveridge, J. Am. Chem. Soc. **106**, 3713 (1984).
[47] P. A. Bergstrom, J. Lindgren and O. Kristiansson, J. Phys. Chem. **95**, 8575 (1991).
[48] R. W. Impey, P. A. Madden and I. R. Mcdonald, J. Phys. Chem. **87**, 5071 (1983).

ISSN 1003-7713/DOI:10.1360/cjcp2007.20(1).22.9